Cochlear macromechanics: Time domain solutions

J. B. Allen and M. M. Sondhi

Acoustics Research Department, Bell Laboratories, Murray Hill, New Jersey 07974
(Received 4 December 1978; revised 28 March 1979)

In this paper we report on a new method of solving a previous derived, two-dimensional model, integral equation for basilar membrane (BM) motion. The method uses a recursive algorithm for the solution of an initial-value problem in the time domain, combined with a fast Fourier transform (FFT) convolution in the space domain at each time step. Thus, the method capitalizes on the high speed and accuracy of the FFT yet allows the BM to have nonlinear mechanical properties. Using the new method we compute (linear) solutions for various choices of model parameters and compare the results to the experimental measurements of Rhode. [J. Acoust. Soc. Am. **49**, 1218–1231 (1971)]. We also demonstrate the effect of including longitudinal stiffness along the BM and conclude that it is useful in matching the high-frequency slope as measured by Rhode.

PACS numbers: 43.63.Bq, 43.63.Kz

LIST OF SYMBOLS

BM	Basilar membrane
ST	Scala tympani
SV	Scala vestibuli
CF	Characteristic frequency
x	Longitudinal (place) coordinate
y	coordinate perpendicular to BM
t	time coordinate
$p(x,t)$	scala pressure
$v(x,t)$	BM velocity
$\xi(x,t)$	BM displacement
$\dot{v}(x,t)$	BM acceleration
d	stapes displacement
u	stapes velocity
$G(x,x')$	Green's function
$F(\sigma)$	see Eq. (5)
L	length of BM
H	height of cochlear scala
ρ	density of cochlear fluids
$W(x)$	BM width
$\mathbf{F}\{\cdot\}$	Fourier transform
M	number of points along BM
m	BM mass
$K(x)$	BM stiffness
$R(x)$	BM damping
Δ	$L/(M-1)$, spatial increment
$b(x,t)$	see Eq. (27b)
$Q(x)$	augmented kernel, Eq. (28).
$\mathfrak{D}$	reduced plate operator Eq. (18)

INTRODUCTION

In this paper we report on a new method for efficiently solving previously developed model equations of basilar membrane (BM) motion. We then report on many new results using this new method which are, for the most part, refinements on previous results. The most important contribution we report on here is our discovery of an efficient and rapid method of numerical solution of the previously developed integral equation. The method takes advantage of the speed and accuracy of fast Fourier transform (FFT) convolution methods and makes essentially *no* approximations other than that of discretizing the integral equation. Furthermore, the solution is in the time domain, making the future inclusion of signal dependent damping (nonlinear mechanics) feasible.

Using our new method, we show results for various model parameters and compare them with the experimental measurements of Rhode. We then demonstrate the effects of introducing longitudinal stiffness along the basilar membrane.

The model equations we have been investigating are formally the same as discussed in Allen (1977a). We assume that the cochlea may be modeled as a two-dimensional rectangular chamber (Fig. 1) filled with an inviscid, incompressible fluid and separated by a homogeneous anisotropic, tapered plate (see Sec. III). The upper and side walls are assumed to be rigid. At the stapes/round window end $x=0$, we assume a uniform velocity, piston source (as the stapes move in, the round window moves out by an equal amount.)

The early cochlear modeling work of Helmholtz ignored fluid coupling, treating the cochlea as a homogeneous, anisotropic tapered membrane. In the late forties, transmission line models were developed in an attempt to approximately account for fluid coupling (Zwislocki, 1948). While these models captured the essence of the mechanical phenomena and are concep-

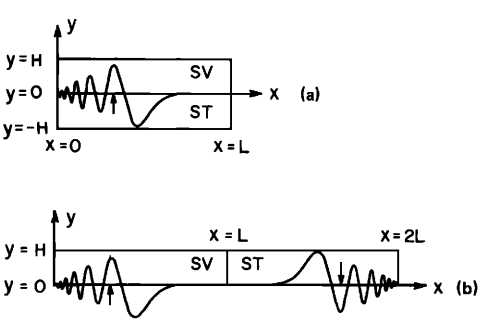

FIG. 1. (a) Geometry of the cochlea. (b) The assumed symmetry of the motion about the helicotrema.

 0001-4966/79/070123-10$00.80 © 1979 Acoustical Society of America

Redistribution subject to ASA license or copyright; see http://acousticalsociety.org/content/terms. Download to IP: 130.126.255.62 On: Thu, 17 Apr 2014 18:17:04

tually very important, they are not quantitatively accurate enough to make detailed comparisons with measurements (Sondhi, 1978). The transmission line models describe the cochlea as a spatially varying transmission line. In these models it is difficult to accurately assess the meaning of various parameters such as chamber depth, BM width, or BM mechanical properties since they do not explicitly appear in the equations. As a result one must be very careful when using this class of models.

I. FLUID MECHANICS OF THE COCHLEA

In the modern models, fluid motion in the cochlea is described independently from the mechanics of the basilar membrane by the use of Green's functions (Allen, 1977a). By Green's theorem, one relates trans-BM pressure to BM acceleration. This fluid equation, along with the plate equation for BM motion, then completely specify BM motion. This approach explicitly accounts for the dependence of the solutions on the geometrical and mechanical parameters. It does not account for coiling, compressibility, scala fluid viscosity, or lateral (radial) fluid motion.

Our previous recent results using the Green's function were restricted to steady-state pure tone responses using linear models. Due to improved understanding of nonlinear phenomena in the cochlea (Kim, Molnar, and Pfeiffer, 1973; Kim and Molnar, 1975; Hall, 1977; Hall, 1974; Hall, 1978), it appears desirable to attempt to incorporate nonlinear (signal dependent) BM properties (e.g., damping) into the fluid mechanical models. This is best achieved with a time domain description of BM motion (rather than using frequency domain methods which rely heavily on linear superposition concepts).

Our first attempt at improved time-domain models was to use the differential equation approximation of Sondhi (1978). However, a time-domain formulation of these equations in a form suitable for computer implementation, while feasible, appears to be quite difficult, and to date, we have not had success with this approach. In reviewing the possible time domain methods at our disposal we discovered that the original integral equation could be solved directly in the time domain in an extremely efficient manner by the use of the fast Fourier transform (FFT).

II. A TIME DOMAIN INTEGRAL EQUATION

In this section we shall review the basic model mentioned earlier. We shall then show that the resulting integral equation may be written as a circular convolution.[1]

As discussed first by Lien (1973), and developed further by Allen (1977a), scala pressure $p(x,t)$ and BM velocity $v(x,t)$ are related through the integral relation

$$p(x,t)=\rho\int_0^L G(x,x')\dot{v}(x',t)dx'+(L-x)\rho\dot{u}(t)\,, \tag{1}$$

where ρ is the fluid density, L the length of the cochlea, G the Green's function, $u(t)$ the stapes velocity, and

$$\dot{v}=\frac{\partial v}{\partial t}=\frac{\partial^2\xi}{\partial t^2}\,, \tag{2a}$$

$$\dot{u}=\ddot{d}=\frac{\partial^2 d}{\partial t^2}\,, \tag{2b}$$

where $d(t)$ is the stapes displacement and $\xi(x,t)$ is the BM displacement.[2] Positive directions for d, v, and ξ are into the upper chamber SV in Fig. 1(a). The scala pressure $p(x,t)$ is referenced to the pressure at the helicotrema ($x=L$). The trans-BM pressure Δp is then $2p$, by symmetry. Derivations of this equation by two different methods may be found in Allen (1977a) and Sondhi (1978). By way of review, $G(x,x')$ is the solution to Laplace's equation for the pressure on the BM($y=0$), at a point x, due to a point source (i.e., a δ function) of acceleration on the BM at x'. In solving for G, the fluid boundary conditions must be identical to those assumed in the undriven cochlear model, namely zero normal velocity at the walls and stapes and zero pressure (and hence velocity) at the apex, $x=L$.

As discussed by Lesser and Berkley (1972), and Allen (1977a), the mathematical description of the problem is simplified by unfolding the cochlea as shown in Fig. 1(b). Here the chamber $0\leq x\leq L$ represents the scala vestibuli (SV), the chamber $L\leq x\leq 2L$ represents the scala tympani (ST), and the surface $y=0$ represents the BM. In this representation the BM impedance must have *even* symmetry around $x=L$ [i.e., $Z(L-x)=Z(L+x)$], while the pressure and BM velocity must have *odd* symmetry around $x=L$. Thus when a point in SV moves up as shown by the small arrow in Fig. 1(b), the corresponding point in ST must move down.

The method of solution that we present in this paper depends on the following further insight:

For $0\leq x\leq 2L$, the motion in the cochlea of Fig. 1(b) is identical to the motion of the periodic extended cochlea, of period $4L$, shown in Fig. 2. Note that $x=0$ is a point of *even* symmetry in this figure. The small arrows show the symmetry of $v(x)$ [which is the same as that of both $\xi(x)$ and $p(x)$] in the extended cochlea. For brevity we will call this symmetry "real-odd harmonic," because the Fourier series expansion of such a periodic function consists only of odd-harmonic cosine terms.

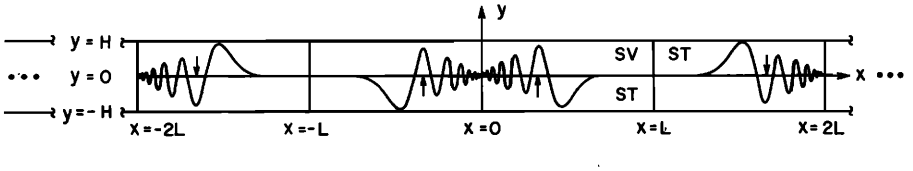

FIG. 2. Extended cochlea showing the $4L$ real-odd harmonic symmetry. This symmetry is used to exactly transform the integral term of the Green's function equation into a periodic convolution, which may be evaluated by Fourier transforms.

Redistribution subject to ASA license or copyright; see http://acousticalsociety.org/content/terms. Download to IP: 130.126.255.62 On: Thu, 17 Apr 2014 18:17:04

This device of replacing a problem by one with periodic boundary conditions is often used in physical modeling. To those familiar with this technique the truth of the above assertion is obvious. To prove it formally, note that $G(x,x')$ in Eq. (1) has a natural periodic extension outside the range $0 \leq (x,x') \leq L$, and has real-odd harmonic symmetry in each of its arguments. Further, $G(x,x')$ may be written as

$$G(x,x') = F(|x-x'|) + F(|x+x'|), \tag{3}$$

where F has real-odd harmonic symmetry. These properties follow from the representation of G in terms of images (Allen, 1977a), as well as from the representation in terms of Jacobian elliptic functions (Sondhi, 1978). From the image representation of G, Allen's Eq. (B4),

$$G(x,x') = \frac{-1}{\pi} \sum_{n=-\infty}^{\infty} \sum_{m=-\infty}^{\infty} (-1)^n \ln(r_{nm}^{+} r_{nm}^{-}), \tag{4a}$$

where

$$r_{nm}^{\pm} = [(x \pm x' + 2nL)^2 + (2mH)^2]^{1/2}. \tag{4b}$$

$r_{nm}^{\pm}$ are the distances from the measurement point at x to the (n,m) image of the source placed at x'. Since

$$\ln(r^{+}r^{-}) = \ln(r^{+}) + \ln(r^{-}),$$

it is easily seen that Eq. (3) is true with

$$F(\sigma) = -\frac{1}{2\pi} \sum_{n} \sum_{m} (-1)^n \ln[\,(|\sigma| + 2nL)^2 + (2mH)^2]. \tag{5}$$

Also the fact that $F(\sigma)$ has real-odd harmonic symmetry is readily verified by direct substitution. It will be convenient to use the double bracket modulo notation indicating an arbitrary function $f(x)$ periodic with period $4L$, whereby $f((x))$ is defined as

$$f((x)) = f(x), \quad -2L < x \leq 2L$$

and for other x values as

$$f((x)) = f(x + 4nL), \quad -2L < x + 4nL \leq 2L,$$

with n any integer. With this notation, and using the symmetries of v, p, and G, Eq. (1) may be written as

$$p((x)) = \frac{\rho}{4} \int_{-2L}^{2L} G(x,x') \dot{v}((x'))\,dx' + ((L - |x|))\rho\dot{u}, \tag{6}$$

or from Eq. (3)

$$p((x)) = \frac{\rho}{4} \int_{-2L}^{2L} [F(x-x') + F(x+x')] \dot{v}((x'))\,dx' + ((L - |x|))\rho\dot{u}. \tag{7}$$

By a simple transformation of variables on the second term in the integral and using the real-odd harmonic symmetry of v [specifically we use $v(x) = v(2L - x)$] and F we find that

$$2p((x)) = \rho \int_{-2L}^{2L} F((x-x')) \dot{v}((x'))\,dx' + 2((L - |x|))\rho\dot{u}. \tag{8}$$

Each term of Eq. (8) is periodic with period $4L$, and therefore may be expanded as a Fourier series. If this were to be done, the Fourier coefficients of the integral term could be written as a product of the Fourier coefficients of F and $\dot{v}$, since the integral is a circular (periodic) convolution. As an alternative approach, we propose spatially sampling each of the functions $p(x)$, $F(x)$, and $v(x)$, giving p_k, F_k, and v_k thereby transforming Eq. (8) into the discrete convolution equation

$$2p_k = \frac{\rho L}{M} \sum_{m=0}^{4M-1} F_{k-m} \dot{v}_m + 2\left(1 - \frac{|k|}{M}\right) L\rho\dot{u}. \tag{9}$$

In this representation p_k, F_k, and v_k are periodic with period $4M$ samples, and if $\Delta = L/(M-1)$, then $p_k = p(k\Delta)$, $F_k = F(k\Delta)$, and $v_k = v(k\Delta)$.

The exact nature of the error made in "sampling" p, v, and F cannot be quantified without studying the high spatial frequencies present in each of these dependent variables. Any frequencies higher than one-half the spatial sampling (Nyquist) frequency will give rise to a type of error called "aliasing." However, if the samples are dense enough (M large enough), Eq. (9) will accurately represent our original Eq. (8). Much of the earlier work has used $M = 175$ samples along the BM length. In this work, we have used $M = 256$ (and under some conditions, $M = 512$) points. For $M = 256$ points, the sum in Eq. (9) represents a 1024-point circular convolution.

Sondhi (1978) has given a simple closed form expression for $F(\sigma)$. After multiplying by $-(1/\pi)$ to account for a difference in definitions, his Eq. (31) gives

$$F(\sigma) = \frac{L - |\sigma|}{2H} - \frac{1}{\pi} \ln[1 - \exp(-\pi|\sigma|/H)], \quad 0 \leq |\sigma| \leq L$$
$$= -F(2L - \sigma), \quad L \leq |\sigma| \leq 2L. \tag{10}$$

The sampled version of this function to be used in Eq. (9) (obtained in the case of $k = 0$ by integrating over the log singularity at $\sigma = 0$) is

$$F_k = \begin{cases} \dfrac{L}{2H} - \dfrac{1}{\pi}\left\{\ln\left(\dfrac{\pi L}{2MH}\right) - 1\right\}, & k = 0 \\ \dfrac{L}{2H}(1 - k/M) - \dfrac{1}{\pi}\ln[1 - \exp(-\pi kL/HM)], & k \neq 0 \end{cases} \tag{11}$$

with $0 \leq k \leq M$. F_k for other ranges of k may be determined by its real-odd harmonic symmetry since

$$F_k = F_{-k} = -F_{2M-k}. \tag{12}$$

One period of F_k is shown in Fig. 3.

III. BASILAR MEMBRANE PLATE EQUATION

The results of the previous section summarize (and extend) the fluid mechanical equations for fluid coupling within the model cochlea. The important assumptions thus far are:

(1) linear *fluid* motion,
(2) two-dimensional flow fields (longitudinal and vertical),
(3) incompressible (∞ speed of sound), inviscid fluid,
(4) a rectangular cochlea,
(5) piston boundary conditions at the stapes and round window, and
(6) zero pressure at the helicotrema.

Redistribution subject to ASA license or copyright; see http://acousticalsociety.org/content/terms. Download to IP: 130.126.255.62 On: Thu, 17 Apr 2014 18:17:04

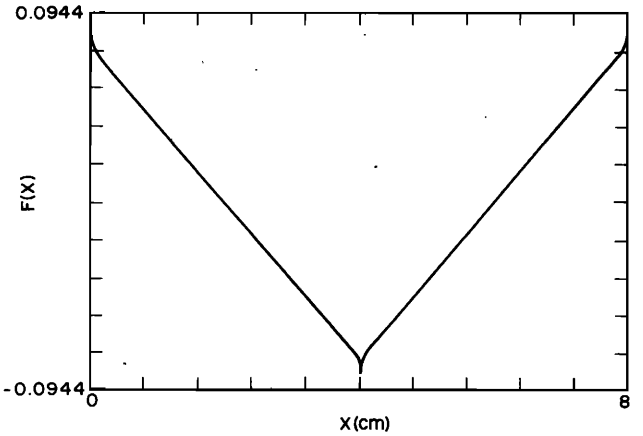

FIG. 3. Plot of the kernel $F(x)$ of the integral equation on the interval $4L$ showing its real-odd symmetry.

Equation (8) relates the pressure $p(x,t)$ in the scala on the BM surface to the acceleration of the BM $\dot{v}=\ddot{\xi}$, where $\xi(x,t)$ is the BM displacement.

We now seek a physical model of the BM displacement $\xi(x,t)$ in terms of the forces across it. Toward this end we expand on the approach of Lien (and Cox) (1973). If the BM is modeled as a homogeneous anisotropic plate [see pp. 365–366 of Timoshenko and Woinowsky-Krieger, 1959] then the basic equation for the plate's displacement is

$$D_x\frac{\partial^4\xi}{\partial x^4}+2(D_xD_z)^{1/2}\frac{\partial^4\xi}{\partial x^2\partial z^2}+D_z\frac{\partial^4\xi}{\partial z^4}=q(x,z,t)\,, \tag{13}$$

where q is the load (force/area) on the plate. The parameters D_x, D_z are assumed to be constants (homogeneity) but not necessarily equal (anisotropy). They are determined by the internal structure, thickness, and modulus of elasticity of the BM.

For the case of the BM, the load q consists of the inertia of the BM mass $m\ddot{\xi}$, BM damping $R(x)\dot{\xi}$, and the trans-BM pressure $2p$ (pressure across the BM). Thus, we have

$$q=-2p-R(x)\dot{\xi}-m\ddot{\xi}\,. \tag{14}$$

A physical model for $R(x)$ has been proposed (Allen, 1978) and further discussion of this topic will be deferred to a future paper. The mass per unit length is that of the organ of Corti and does not include the fluid of the cochlear duct since Reissner's membrane is ignored in this formulation. If we use the shorthand vector notation for Eq. (13)

$$\mathbf{D}\cdot\nabla^4\xi=q\,,$$

then Eq. (14) may be written

$$p=-\frac{1}{2}[\mathbf{D}\cdot\nabla^4\xi+R(x)\dot{\xi}+m\ddot{\xi}]\,. \tag{15}$$

At this point we might have obtained an equation for BM displacement by equating the pressure p of Eq. (15) to that of Eq. (8), except that Eq. (8) has been derived on the assumption that in the z (lateral or radial) dimension there is no variation. We must therefore first find a two-dimensional approximation to Eq. (15).

IV. REDUCTION OF THE PLATE EQUATION TO TWO DIMENSIONS

In order to eliminate the z dependence in Eq. (15) we assume that the pressure is uniformly distributed in the z direction and that the z dependence of the BM displacement has a simple cos(·) dependence across the BM width $W(z)$ (Lien, 1973; Allen, 1977a). If $\xi(x,0,t)$ is the centerline BM displacement, we assume that

$$\xi(x,z,t)=\xi(x,0,t)\cos[\pi z/W(x)]\,. \tag{16}$$

This *approximate* transformation allows us to neatly reduce Eq. (15) to a function independent of z in terms of the BM centerline displacement $\xi(x,0,t)$ since by Eq. (16) [and ignoring all derivatives of $W(x)$]

$$\left.\frac{\partial^4\xi}{\partial z^4}\right|_{z=0}=\left(\frac{\pi}{W(x)}\right)^4\xi(x,0,t)\,, \tag{17a}$$

$$\left.\frac{\partial^4\xi}{\partial x^4}\right|_{z=0}=\frac{\partial^4\xi}{\partial x^4}(x,0,t)\,, \tag{17b}$$

$$\left.\frac{\partial^4\xi}{\partial x^2\partial z^2}\right|_{z=0}=-\left(\frac{\pi}{W(x)}\right)^2\frac{\partial^2\xi}{\partial x^2}(x,0,t)\,. \tag{17c}$$

By use of this approximation it is possible to greatly simplify our equation without, we hope, ignoring any significant physical properties.

Thus, Eq. (13) for the (two-dimensional) BM plate equation evaluated on $z=0$ becomes after utilizing Eq. (17)

$$\mathfrak{D}\xi=D_x\frac{\partial^4\xi}{\partial x^4}-2(D_xD_z)^{1/2}\left(\frac{\pi}{W(x)}\right)^2\frac{\partial^2\xi}{\partial x^2}+D_z\left(\frac{\pi}{W(x)}\right)^4\xi\,. \tag{18}$$

Substituting $\mathfrak{D}\xi$ into Eq. (15) for $\mathfrak{D}\cdot\nabla^4\xi$ and then substituting for p from Eq. (8) gives

$$\mathfrak{D}\xi+R(x)\dot{\xi}+m\ddot{\xi}=-\rho F*\ddot{\xi}-2((L-|x|))\rho\dot{u}\,, \tag{19}$$

which is the required equation for BM motion. The * denotes the circular convolution integral of Eq. (8), a convolution which can be carried out because the argument of F is invariant to shifts of $4L$. The invariance results from the assumptions of constant scala height H and BM mass m.

Equation (19) is an initial value problem in time and a boundary value problem in space. We will solve the boundary value problem by Fourier transforms, and the initial value problem recursively starting from the initial displacement and velocity of the membrane. The Fourier transforms and the updates at each time step alternate during the solution procedure, as will become clear in the following discussion.

V. DISCRETIZING THE SPACE AND TIME VARIABLES

In this section we show how we discretize x and t of Eq. (19). The right-hand side has already been shown in Eqs. (9) and (11) with x discretized to the values $0,\Delta,\ldots,(4M-1)\Delta$, where $\Delta=L/(M-1)$ is the spatial sampling interval. To complete the x discretization we specify that the partial derivatives $\xi_{xx}=\partial^2\xi/\partial x^2$,

Redistribution subject to ASA license or copyright; see http://acousticalsociety.org/content/terms. Download to IP: 130.126.255.62 On: Thu, 17 Apr 2014 18:17:04

$\xi_{xxxx} = \partial^4\xi/\partial x^4$ occurring in Eq. (18) be replaced by the central differences

$$\xi_{xx} \Longleftrightarrow (\xi_{k-1,n} - 2\xi_{k,n} + \xi_{k+1,n})/\Delta^2, \tag{20}$$

$$\xi_{xxxx} \Longleftrightarrow (\xi_{k-2,n} - 4\xi_{k-1,n} + 6\xi_{k,n} - 4\xi_{k+1,n} + \xi_{k+2,n})/\Delta^4, \tag{21}$$

where k is the space variable and n is the time variable.

In computing the terms ξ_{xx} and ξ_{xxxx}, boundary conditions (BC) are necessary at $x = 0$ and $x = L$, the stapes and helicotrema. Since we assume that D_x is small, the actual BC's used are probably unimportant. We have used the condition that ξ_{xxxx} and ξ_{xx} are zero in the neighborhoods of $x = 0$ and $x = L$. Periodic boundary conditions would be the natural choice, but for computational reasons these conditions were not used here. When one is not interested in the effects of longitudinal stiffness (i.e., when $D_x = 0$), most of the assumptions in this section about Eq. (13) are not required.

The discretization in time is achieved similarly by specifying the time derivatives in terms of sampled values. We specify that any time function $g(t)$ and its time derivatives be approximated by the following differences:

$$\begin{aligned} \ddot{g}(t) &\Longleftrightarrow (g_n - 2g_{n-1} + g_{n-2})/T^2, \\ \dot{g}(t) &\Longleftrightarrow (g_{n-1} - g_{n-2})/T, \\ g(t) &\Longleftrightarrow g_{n-1}, \end{aligned} \tag{22}$$

where T is the sampling interval and n is the discrete time variable. The reason for this choice is based on the behavior of a constant coefficient second-order differential equation.

For example suppose we were given the second-order differential equation (23a) having Laplace transform (23b) and roots s_+ and s_- (23c)

$$\ddot{g} + a\dot{g} + bg = f(t), \tag{23a}$$

$$(s^2 + as + b)G(s) = F(s), \tag{23b}$$

$$(s - s_+)(s - s_-)G(s) = F(s). \tag{23c}$$

When we map the derivatives of Eq. (23a) by differences, as in Eq. (22), it reduces to the recursion relation

$$\begin{aligned} g_n &= (2 - aT - bT^2)g_{n-1} - (1 - aT)g_{n-2} + T^2 f_{n-1} \\ &= -2\alpha g_{n-1} - \beta^2 g_{n-2} + T^2 f_{n-1}. \end{aligned} \tag{24}$$

This discrete equation has the z transform

$$(1 + 2\alpha z^{-1} + \beta^2 z^{-2})G(z) = z^{-1}T^2 F(z). \tag{25}$$

The two characteristic roots z_+ and z_- of the difference Eq. (25) are

$$z_\pm = (1 - aT)^{1/2}\exp(\pm i\theta_0), \tag{26a}$$

where

$$\cos\theta_0 = \frac{2 - aT - bT^2}{2(1 - aT)^{1/2}}. \tag{26b}$$

When $|z_\pm| < 1$, the difference equation is stable and the root locations describe the resonant frequencies of the difference equation. By studying root locus plots of $z_\pm(s_+, s_-)$ as a function of the roots s_+ and s_- of Eq. (23c) in the s plane, one may study the mapping implied by the differencing scheme of Eq. (22). From this analysis it is possible to show that to guarantee stable difference equations, the sampling frequency $1/T$ must be at least π times greater than the resonant frequency of Eq. (23b). Equation (22) turns out to be an excellent (the best to our knowledge) method of transforming our differential equation in the sense that the digital resonances $z_\pm$ closely approximate the actual resonances $s_\pm$ [in the sense of *impulse invariance* (Rabiner and Gold, 1975)].

VI. METHOD OF SOLUTION

By using the transformed Eqs. (9), (11), (20), (21), and (22) we render Eq. (19) discrete in x and t. For a fixed time $t/T = n$, this discretized equation is a relationship between the vector of displacements $\boldsymbol{\xi}_n$ (with components $\xi_{n,m}, m = x/\Delta = 0, 1, \ldots M - 1$) and the vectors $\boldsymbol{\xi}_{n-1}$ and $\boldsymbol{\xi}_{n-2}$. We can now solve recursively for each new vector $\boldsymbol{\xi}_n$ in terms of the previously computed vectors. In the continuous time domain this is equivalent to rearranging Eq. (19) with the $\ddot{\xi}$ terms on the left

$$\rho F * \ddot{\xi} + m\ddot{\xi} = b(x, t), \tag{27a}$$

where

$$b(x, t) = -\mathfrak{D}\xi - R(x)\dot{\xi} - 2((L - |x|))\rho\dot{u}. \tag{27b}$$

Defining an augmented kernel $Q(x)$ as

$$Q(x) = \rho F(x) + (m/2)[\delta(x) - \delta(2L - x)], \tag{28}$$

where $\delta(x)$ is the Dirac δ function, Eq. (27) may be rewritten as

$$Q(x) * \ddot{\xi}(x) = b(x, t), \tag{29}$$

where * represents circular convolution. In Eq. (28) the factor of one-half and the second $\delta(\cdot)$ term are necessary to make $Q(x)$ have the real-odd harmonic symmetry required by the circular convolution. Because of the known symmetry of ξ, this modification is exact, as may easily be shown by direct substitution.

For a fixed time t, this equation may be solved by a Fourier transformation which converts the circular convolution into a multiplication. Thus,

$$\ddot{\xi}(x, t) = \mathbf{F}^{-1}\left(\frac{\mathbf{F}\{b(x, t)\}}{\mathbf{F}\{Q(x)\}}\right), \tag{30}$$

where $\mathbf{F}\{\cdot\}$ and $\mathbf{F}^{-1}\{\cdot\}$ are the Fourier transform and its inverse. (Recall that in the discrete case this transform is over $4M = 1024$ points. Our hardware array processor is capable of a floating point transform of this size in 9 ms).

By utilizing the real-odd harmonic symmetry of all the functions involved, it is trivial to reduce the transform to a 512 point[3] real FFT (which on our array processor takes 5 ms).

We summarize our method of solution as follows:

(a) Compute $b_{m,n}$ Eq. (27b) at time $n = t/T$ for $m = x/\Delta = 0, \ldots, M - 1$. This requires only previously computed values.

Redistribution subject to ASA license or copyright; see http://acousticalsociety.org/content/terms. Download to IP: 130.126.255.62 On: Thu, 17 Apr 2014 18:17:04

(b) Take the Fourier transform of $b_{m,n}, m = x/\Delta = 0, \ldots, 4M-1$.
(c) Divide by $\mathbf{F}(Q_m)$ (which has been previously computed and stored).
(d) Inverse transform results of c.
(e) Compute a new displacement vector recursively from the discrete version of Eq. (30).
(f) Repeat steps (a)–(e) as often as desired.

The computation time per time step is that required to compute $b(x,t)$, one Fourier transform, one inverse transform and a few vector additions. In the case $D_x = 0$ for which

$$\mathfrak{D}\xi = K(x)\xi(x,t) \tag{31}$$

(i.e., the usual BM stiffness term), we require about 40 ms/time step on our array processor ($M = 256$). This is less than the time required to compute a time step for the one-dimensional transmission line approximation using FORTRAN code.

Note further that the BM mechanical properties need not be linear. The quantity $b(x,t)$ can be any nonlinear function of ξ and $\dot{\xi}$ and the method is still applicable. However, the BM mass m and the scala height H must be constant for the method to apply.

VII. DISCUSSION OF NUMERICAL RESULTS

In order to check our numerical results we solved the case of a constant BM impedance and compared the solutions to an analytical formulation by the normal mode method. The two solution methods differed in the 4th decimal place. We also compared the new method to our previous method (Allen, 1977a) (correcting for the factor of two error mentioned in Footnote 2) and the agreement was excellent. Next we modified the kernel function $F(\sigma)$ of Eq. (10) to be that of the transmission line model [by replacing the $\ln(\cdot)$ term by a δ function] and compared the solutions to the transmission line equation solutions. The agreement again was excellent (the solutions differed by much less than 1 dB). Finally, when either T or Δ were reduced, no changes were observed in the solutions.

We now present the results of simulations. In the first example we assume that D_x, the longitudinal stiffness, is zero, and we compare our numerical results to the measurements of Rhode on squirrel monkey. In making these comparisons, in order to be consistent with Rhode, it is necessary to redefine the direction of BM motion with displacement into ST as positive.

Our present comparisons differ from earlier ones in several respects. First we have attempted to model cochlear map data. Second we have not arbitrarily scaled the magnitude of the transfer function. The measured data is a transfer ratio between malleus and BM velocity. We have modeled the BM to stapes ratio. The malleus to stapes response is believed to be a flat attenuation of about 6 dB for squirrel monkey. We did not correct for this effect here. Third we attempted to match the phase slope below CF. As a result of these three constraints the damping was the only remaining unspecified parameter. This was then varied to give the best fit near CF. For squirrel monkey we choose the following parameters[4] (in cgs units)

$$\rho = 1(\mathrm{g/cm^3}),\quad L = 2.5(\mathrm{cm}),\quad H = 0.097(\mathrm{cm}),$$

$$T = 0.25\times 10^{-5}(\mathrm{s}),\quad a = 0.9(\mathrm{cm^{-1}}),\quad m = 0.043(\mathrm{g/cm^2}),$$

$$R(x) = 100(\mathrm{dyn\text{-}s/cm^3}),$$

$$W(x) = 0.017\exp[0.5(ax + 0.031x^5)](\mathrm{cm}),$$

$$D_z = K_0 W^4(0)/\pi^4(\mathrm{dyn\,cm}),\quad K_0 = 0.262\times 10^{10}(\mathrm{dyn/cm^3}),$$

$$D_x = 0,\quad M = 512(\mathrm{points}).$$

Note that R is a constant here. The parameter a is called the cochlear map parameter and determines the slope of the cochlear map.

In Fig. 4(a) and 4(b) we show a comparison of our calculated results with some data of Rhode (1971, Fig. 6). The numbers 1–10 code the BM measurement points. The actual locations may be determined by reference to Fig. 4(e). The calculated frequency response was obtained by (time) Fourier transforming (by FFT) the normalized time velocity (impulse) response $\dot{\xi}(x_0,t)/u_0$ (normalized by the stapes velocity u_0) at a place $x = x_0$ on the model BM to an impulsive velocity input

$$\dot{d}(t) = u_0\delta(t). \tag{32}$$

In Figs. 4(c) and 4(d) we increased the damping R to $R = 1000$. In Figs. 4(a) and 4(b) the magnitude gives a better match than the phase, while the reverse is true in Figs. 4(c) and 4(d). We were not able to obtain simultaneous matches to both magnitude and phase with one choice of R.

In Fig. 4(e) we show the calculated cochlear map for the parameters assumed along with three estimated[5] values for squirrel monkey (SQM). The cochlear map is a plot of $\log_{10}(f_{CF})$ against x_{CF}, the place of measurement. For squirrel monkey the cochlear map has not been measured. Our lack of knowledge of the SQM cochlear map makes further comparisons to Rhode's data difficult (if not impossible). Our unusual choice of $W(x)$ causes the computed map to be curved.

In Fig. 5(a) and 5(b) we show the results of similar comparisons to Fig. 8 of Rhode (1971) (higher CF data). In Fig. 5(a) and 5(b)

$$D_z = K_0(W(0)/\pi)^4(\mathrm{dyn\text{-}cm}),\quad D_x = 0,$$

$$W(x) = 0.017\exp[0.5ax]\,\mathrm{cm},\quad K_0 = 0.28\times 10^{10}(\mathrm{dyn/cm^3}),$$

$$R_0 = 200(\mathrm{dyn\text{-}s/cm^3}),\quad m_0 = 0.032(\mathrm{g/cm^2}),$$

$$a = 1.5(\mathrm{cm^{-1}}),\quad L = 4(\mathrm{cm}),\quad H = 0.13(\mathrm{cm}),$$

$$T = 0.5\times 10^{-5}(\mathrm{s}),\quad M = 256(\mathrm{points}).$$

For Fig. 5(c) the damping was increased by a factor of 5 to $R = 1000$. The cochlea map for the case of $R = 200$ is given in Fig. 5(d), again along with some estimated relative cochlear map points for SQM. We feel that the cochlear map is an important constraint on the model since it determines a.

In Fig. 6 we show the results of including longitudinal stiffness into the model. In this example all conditions were identical to those of Fig. 4(a) except that $D_R = 10^{-4}$

Redistribution subject to ASA license or copyright; see http://acousticalsociety.org/content/terms. Download to IP: 130.126.255.62 On: Thu, 17 Apr 2014 18:17:04

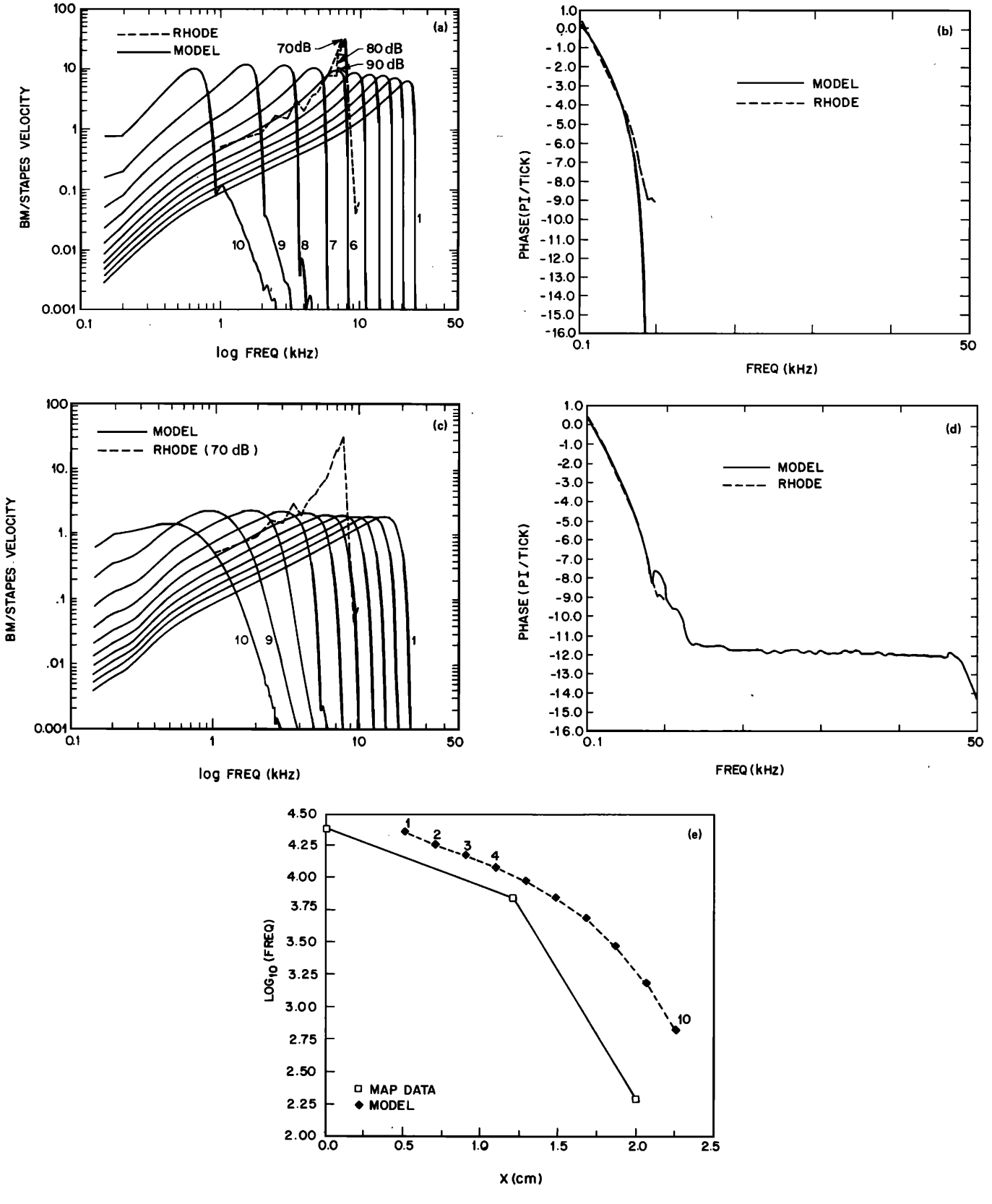

FIG. 4. Results of solving Eq. (19) for the BM/stapes velocity transfer function: (a) magnitude of velocity ratios; (b) phase with parameters given in Sec. VII; (c) magnitude with the damping increased to $R=1000$; (d) phase for case of increased damping; and (e) cochlear map from model. In (e) the solid line connects three rough estimates of the squirrel monkey map. These points may be shifted along the x axis since they are only relative positional estimates. Note that we have effectively made the scala length greater than the BM length, which is believed to be only 2 cm long. The scala length for squirrel monkey is presently unknown. The dashed plots in (a)–(e) are Rhode's 69–473 squirrel monkey data for 70, 80, and 90 dB SPL. For all phase plots the sign of BM displacement was reversed in order to be consistent with Rhode's data where displacements into ST are positive.

Redistribution subject to ASA license or copyright; see http://acousticalsociety.org/content/terms. Download to IP: 130.126.255.62 On: Thu, 17 Apr 2014 18:17:04

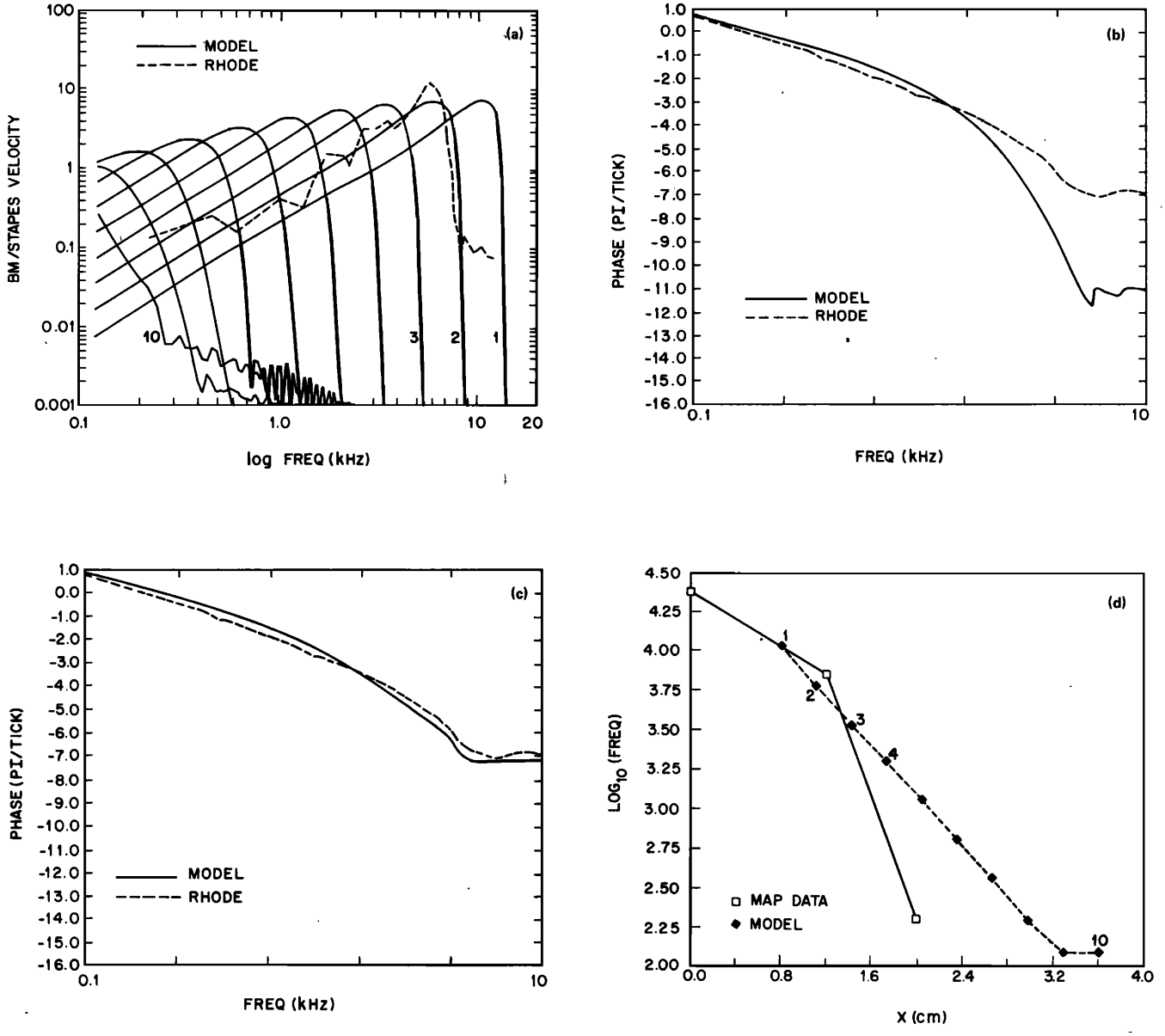

FIG. 5. In this figure we compare our model results to Rhode's 1971, Fig. 8 data (higher CF plot): (a) family of transfer functions and Rhode's data, (b) phase, (c) phase with fivefold increase in damping, and (d) cochlear map. The important difference between this case and the previous one is that we have arbitrarily chosen a very different cochlear map parameter $a = 1.5$ (compared to the previous case of $a = 0.9$) and the cochlear map has been made linear by our choice of $K(x) = K_0 e^{-2ax}$ [when R is small, f_{CF} is always very well approximated by $2\pi f_{CF} = \sqrt{K(x)/m}$]. Due to the range of CF's required, and our choice of a, the length was chosen to be 4 cm. Since the squirrel monkey basilar membrane is only 2 cm long, the cochlear map of the previous figure is more reasonable than the one shown here. In general the BM velocity is only weakly dependent on a. Measurements are needed of squirrel monkey cochlear maps. As in the previous figure, it was necessary to increase R in order to match the phase. Thus we were not able to match both magnitude and phase with one choice of R.

and 10^{-5}, where $D_R = D_x/D_z$. According to these results, D_x must be less than 10^{-4} times smaller than D_z, the transverse stiffness coefficient. This result argues strongly against models which assume significant BM longitudinal stiffness. The phase for this case differs only above f_{CF}, and has a smaller slope in that region.

In all cases where we found reasonable agreement between the measured data and the model, the high-frequency ($f > f_{CF}$) plateau as observed by Rhode was not present in the model results. The reason for this difference is presently unknown. Note that the plateau is present for lower CF's, Fig. 4(a).

VIII. PARAMETER SELECTION

In order to help fit measured data for frequencies f below the characteristic frequency (f_{CF}) we have used the following approximate formulas for m and H obtained from the one-dimensional model (Sondhi, 1978, Eq. 42) and the WKB approximation [Morse and Feshbach, (1953), p. 1092]

$$m = \frac{4\rho}{\tau_0 \omega_0 G_0} \frac{\sinh(0.5 a x_0)}{a}, \tag{33}$$

$$H = m G_0^2 e^{-a x_0}/2\rho, \tag{34}$$

Redistribution subject to ASA license or copyright; see http://acousticalsociety.org/content/terms. Download to IP: 130.126.255.62 On: Thu, 17 Apr 2014 18:17:04

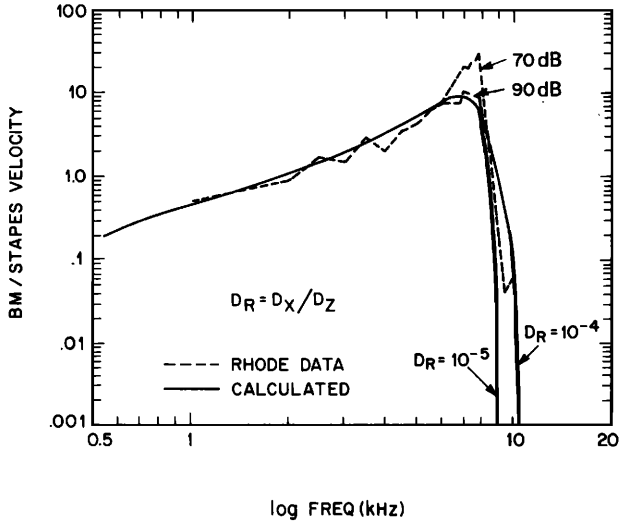

FIG. 6. In this figure we compare the model results to Rhode's data showing the effect of a stiffness ratio $D_R = 10^{-4}$ and 10^{-5}, where $D_R = D_x/D_z$. Apparently even minute amounts of longitudinal stiffness strongly modify the high-frequency slope. Except for the longitudinal stiffness, all conditions are identical to those of Fig. 4(a). Note the expanded frequency scale of this plot.

where we define

$\omega = 2\pi f$, $\omega_0 = 2\pi f_{CF}$,

x_0 = place of measurement relative to stapes,

a = map parameter.

τ_0 is the phase slope for frequencies well below CF

$$\tau_0 = \left| \frac{\partial \phi}{\partial \omega} \right|_{\omega < \omega_0}, \tag{35}$$

as measured at $x = x_0$, and

$$G_0 = \frac{\omega_0}{\omega} \left| \frac{v(x_0, \omega)}{u(\omega)} \right|_{\omega < \omega_0}. \tag{36}$$

For Rhode's 1969 data animal 69-473,

$$f_{CF} = 7785 \text{ Hz}, \quad \tau_0 \approx 0.4 \times 10^{-3} \text{s}, \quad G_0 \approx 4.78, \tag{37}$$

as may be easily determined from his data. The parameters a and x_0 are presently unknown for SQM. We have assumed here that $a = 0.9$ and $x_0 = 1.8$. The use of Eqs. (33) and (34) assure that for frequencies below CF the gain and phase will match measured values. These formulas are therefore very helpful in parameter selection. When the damping R is large, these equations will not be accurate and some other method of parameter selection must be used.

After the determination of H and m, K_0 the stiffness constant, may be estimated from

$$f_{max} = f_{CF}\, e^{ax_0}, \quad K_0 = m(2\pi f_{max})^2. \tag{38}$$

The above formulas should serve only as initial parameter estimates with final refinements made by direct comparison of the computed solution with the experimental results. In most cases we found them to work well.

IX. CONCLUSIONS

In this paper we have presented a method for numerically solving the fluid mechanical equations for basilar membrane motion. The solution proceeds in the time domain and will allow for nonlinear BM parameters (such as signal dependent damping). As a further extension, we have included longitudinal stiffness. As a result of our calculations, large amounts of longitudinal stiffness appear to be inconsistent with Rhode's measurements in squirrel monkey cochleas. This is an important (negative) result because a number of previous cochlear models have assumed significant longitudinal stiffness.

Since our method of solution requires the use of a fast FFT, our solution technique might not be as useful to those who do not have a high speed array processor capable of computing a 512-point real (or 128-point complex, if all symmetry is used) FFT in less than 20 ms. For those without array processors, symmetry may be used to reduce the computation (Rabiner, 1979).

Using very reasonable mechanical parameters we have found reasonable agreement between the model solutions and the measurements of Rhode. The damping required to match the magnitude was different from that needed to match the phase.

If the BM mechanical damping R is nonlinear, as many believe it is, then one would not expect to be able to match Rhode's magnitude and phase with one value of R, since his measurements have been made using different input levels (and hence, different R values, according to the present nonlinear models). Thus we believe that any future model work must include nonlinear damping effects as required by two-tone suppression models (Kim and Molnar, 1975; Hall, 1978). The method of solution presented in this paper is still valid for the case of nonlinear damping. Further refinement in matching the BM magnitude data might be possible if we had more direct data on the SQM cochlea map and Rhode's place of measurement.

The results reported on here continue to support the need for a second filter since the model mechanical response is not as sharply tuned as neural tuning curves (Allen, 1977b).

[1] Circular convolution has the well-known property that it may be performed in $N \log_2 (N)$ time on a digital computer by use of fast Fourier transforms (FFT's), whereas by direct computation, circular convolution takes N^2 time units, where N is the number of points to be convolved. Furthermore, as a result of the circular convolution, storage may be reduced from N^2 to N. These two improvements render the direct solution of the integral equation a trivial matter. The development of the FFT made convolution a practical computer computation for systems where N is greater than a few hundred points.

[2] In Allen (1977a), a factor of two error was made in his Eq. (12). Because of the definition of $G_{BM}(x, x')$, S' of Appendix D should have been from 0 to L rather than 0 to $2L$. Thus the limits on the second integral of Eq. (D11) should have been 0 to L, as shown, but with no factor of two preceding the integral. Making this correction, and using the definition of pressure, $p = i\omega\rho\phi$, Allen's Eq. (12) becomes our present

Redistribution subject to ASA license or copyright; see http://acousticalsociety.org/content/terms. Download to IP: 130.126.255.62 On: Thu, 17 Apr 2014 18:17:04

Eq. (1) above. If all his impedance values Z are normalized by this factor of two, the results of that paper are correct. The statement by Sondhi (1978) after his Eq. (31), p. 1471, becomes correct after this change, and his Eqs. (30) and (31) are then equivalent to Allen's.

[3]By further use of all the symmetries, it is possible to reduce the size to a 256 point real, or 128 point complex FFT. This has been accomplished by L. R. Rabiner (1979). However the complexity of the pre- and postprocessing required is rather cumbersome on our array processor.

[4]All impedances given here are BM impedance values defined by the relation $2p(x,\omega) = -Z(x,\omega)v(x,\omega)$, where $Z(x,\omega) = K(x)/i\omega + R(x) + i\omega m$, and $K(x) = D_g(\pi/W(x))^4$. Note the factor of two difference between this definition of Z and the one used by Allen (1977a) and Sondhi (1978).

[5]The center point was given to us by Rhode (personal communication). The extreme points were estimated from neural data as the highest and lowest possible CF. These points are only relatively estimated. Thus they may be moved along the x axis for best fit.

Allen, Jont, B.(1977a). "Two-dimensional Cochlear Fluid Model: New Results," J. Acoust. Soc. Am. 61, 110–119.

Allen, Jont, B. (1977b). "Cochlear micromechanics–a mechanism for transforming mechanical to neural tuning within the cochlea," J. Acoust. Soc. Am. 62, 930–939.

Allen, Jont, B. (1978). "A physical model of basilar membrane dissipation," J. Acoust. Soc. Am. 63, S43(A).

Hall, J. L. (1974). "Two-tone distortion products in a nonlinear model of the basilar membrane," J. Acoust. Soc. Am. 56, 1818–1828.

Hall, J. L. (1977). "Two-tone suppression in a nonlinear model of the basilar membrane," J. Acoust. Soc. Am. 61, 802–810.

Hall, J. L. (1978). "Model study of Zwicker's "masking period patterns," J. Acoust. Soc. Am. 64, 473–477.

Kim, D. O., Molnar C. E., and Pfeiffer, R. R. (1973). "A System of Nonlinear Differential Equations Modeling Basilar-Membrane Motion," J. Acoust. Soc. Am. 54, 1517–1529.

Kim, D. O., and Molnar, C. E. (1975). "Cochlear Mechanics: Measurements and Models," in *The Nervous System*, edited by D. B. Tower (Raven, New York).

Lesser, M., and Berkley, D. A. (1972). "Fluid mechanics of the cochlea," J. Fluid Mech. 51, 497–512.

Lien, M. (1973). "A Mathematical Model of the Mechanics of the Cochlea," PhD dissertation, Seven Inst. of Wash. Univ., St. Louis, MO (J. R. Cox advisor) (unpublished).

Morse, P. M., and Feshbach, H. (1953). *Methods of Theoretical Physics* (McGraw-Hill, New York), Vol. II.

Rabiner, L. R., and Gold, B. (1975). *Theory and Application of Digital Signal Processing* (Prentice-Hall, Englewood Cliffs, NJ), pp. 212–219.

Rabiner, L. R. (1979). "FFT Subroutines for Sequences with Special Properties," in *IEEE Press Book on Digital Signal Processes* (IEEE Press, New York, NY).

Rhode, W. S. (1971). "Observations of the Vibration of the Basilar Membrane in Squirrel Monkeys using the Mössbauer Technique," J. Acoust. Soc. Am. 49, 1218–1231.

Sondhi, M. M. (1978). "Method for computing motion in a two-dimensional cochlear model;" J. Acoust. Soc. Am. 63, 1468–1477.

Timoshenko, S., and Woinowsky-Krieger, S. (1959). *Theory of Plates and Shells* (McGraw-Hill, New York).

Zwislocki, J. J. (1948). Acta Oto-Laryngol. Suppl. 72.

Zwislocki, J. J. (1950). "Theory of acoustical action of the cochlea," J. Acoust. Soc. Am. 22, 778–784.

Redistribution subject to ASA license or copyright; see http://acousticalsociety.org/content/terms. Download to IP: 130.126.255.62 On: Thu, 17 Apr 2014 18:17:04